Macromolecular Chemistry and Physics
www.mcp-journal.de

Poly(ε-caprolactone) and Poly(ω-pentadecalactone)-Based Networks with Two-Way Shape-Memory Effect through [2+2] Cycloaddition Reactions

*Florence Pilate, Gregory Stoclet, Rosica Mincheva, Philippe Dubois, and Jean-Marie Raquez**

In this work, the synthesis and characterization of triple-shape and two-way shape-memory effect of novel poly(ester-urethane)s (PURs) made of a poly(ε-caprolactone) (PCL) and poly(ω-pentadecalactone) (PPDL) segments and *N*,*N*-bis(2-hydroxyethyl)cinnamide (BHECA) monomer by reactive extrusion (REx) is reported. PCL and PPDL are chosen as semicrystalline segments because of their inherent ability to undergo tensile elongation upon cooling, as prerequisite for the two-way shape-memory effect. BHECA is used as the "cross-linker" due to its ability to participate in reversible [2+2] cycloaddition reaction and to mainly maintain the crystalline features of semicrystalline precursors within these PURs. This novel simple strategy is considered extremely versatile and adaptive because of the possibility to vary crystallizable segments and coupling agents, thus paving the way to the design of a multitude of triple (or more) shape-memory polymers with two-way behavior. Feasibility with PURs containing PCL, PPDL, and BHECA is demonstrated by adjusting the shape-memory behavior (one and two-way effects), and studying the structure–property relationships of the resulting PURs by DSC, DMTA, and 2D wide angle X-ray scattering analyses while varying the weight composition of the two semicrystalline segments.

1. Introduction

Shape-memory polymers (SMPs) are well-known as high-performance materials, with potential applications ranging from biomedical materials to engineering thermoplastics. Initially, the development of SMPs was mostly driven by the biomedical field whereby their ability to pass from a temporary to a permanent shape upon an external stimulus enables applications as stimuli-responsive implants. Most of SMPs are heat-responsive materials and constructed with a switching domain related to glass transition (T_g) or melting temperature (T_m), and a permanent domain formed by a chemical or physical network to ensure cohesion and stability of the whole system during shape-memory process.[1] Transition from an initial (or permanent) shape to a temporary shape can be obtained after deformation at a temperature above T_g or T_m and stabilized upon cooling under a constant loading. After the heating, the polymers spontaneously recover their original shape due to the entropic relaxation of polymer chains. Unless a new programming process is applied, the material remains in this last state without possibility to get any other temporary shape. Such one-directional shape-changing behavior is known as one-way shape-memory effect (1W-SME).[2] There is nowadays a growing interest to more advanced domains like smart textiles,[3] aerospatiale devices,[4,5] and so on via the utilization of complex SMPs.[2] The recent research shows new interesting breakthroughs over complex SMPs: multi-SMPs which are able to display more than one shape transition[6] and two-way (2W)-SMPs exhibiting reversible actuation between temporary and permanent shapes. For example, triple (t)-SMPs change their first temporary shape (A) to a second one (B) followed by third shape (C) upon a step-by-step temperature increase. Two or more temporary shapes can be displayed by designing crosslinked networks with two (or more) segregated phases (e.g., different polymer segments) with distinct T_g or T_m[7–14] or by elaboration of systems having a broad transition temperature.[15–17] Most of them fall in the category of 1W-SMPs since a repeatable programming step is always required. Interestingly, the discovery of the 2W-SME has created more opportunity to these materials as polymeric actuators are able to act as "artificial muscles."[18,19] For these smart materials, an interconversion between temporary and original shapes can be simply achieved upon heating or cooling cycles with an external stress or not.[20] Generally, this behavior is due to reversible polymer chain conformations. Dimension changing under low

Dr. F. Pilate, Dr. R. Mincheva, Prof. P. Dubois, Dr. J.-M. Raquez
Laboratory of Polymeric and Composite Materials (LPCM)
Center of Innovation and Research in Materials and Polymers (CIRMAP)
University of Mons – UMONS
Place du Parc 23, B-7000 Mons, Belgium
E-mail: jean-marie.raquez@umons.ac.be
Dr. G. Stoclet
Université de Lille Nord de France
UMR CNRS 8207
Unité Matériaux et Transformations
Université Lille1 Sciences et Technologies
Bâtiment C6, 59655 Villeneuve d'Ascq, France

DOI: 10.1002/macp.201700345

stresses[21] and reversible actuation between both permanent and temporary states was first demonstrated in liquid crystalline elastomers (LCEs)[18,22] and more recently investigated in glass-forming polydomain nematic-[20] or semicrystalline networks.[23–25] In the case of semicrystalline networks, 2W-SME can be obtained upon crystallization-induced elongation (CIE) and melting-induced contraction (MIC) phenomena related to the presence of highly dense cross-links. In 2008, Chung et al. observed that their cross-linked poly(cyclooctene) films readily undergo tensile elongation upon cooling and inversely, a contraction when the film is heated, both under stretching.[25]

Although semicrystalline polymers, in association or not, seem to be good candidates for 2W-SME due to their vast availability, some of us pointed out the rather limited works published in the realm.[26] This can be explained by the fact that if covalently crosslinked systems derived from semicrystalline precursors are used,[27,28] the permanent cross-linking alters the molecular motion and crystallization phenomena, leading to, in most cases, systems of lower degree of crystallinity and T_m with respect to the non-crosslinked polymeric precursors. In order to overcome this problem, Raquez et al. proposed the elaboration of semicrystalline networks made of thermoreversible [4+2] Diels–Alder cycloadducts.[26] Such reversible cycloaddition reactions enabled the control over the microstructure and therefore the physical properties of the resulting networks, preserving the crystalline features of the networks. Thus, thermoreversible semicrystalline PCL-based networks with high-performance 2W-SME were readily obtained by reactive extrusion.

In a more recent study, some of us reported a simple pathway to the first example of dual heating- and light-responsive PCL-based SME without any overlapping effects between both stimuli.[29] For so doing, heating-responsive PCL-based segments and photo-responsive monomer were coupled using an aliphatic diisocyanate as coupling agent to form poly(ester-urethane)s (PURs). The chain-extension reaction leading to PURs was carried out by reactive extrusion. For photo-responsive SME, *N,N*-bis(2-hydroxyethyl) cinnamide (BHECA) was selected due to the presence of a pendant cinnamide moiety undergoing photoreversible [2+2] cycloaddition reactions in function of a certain wavelength (λ_{switch} = 254 nm).[30] PCL served as a semicrystalline segment ensuring the permanent domains. In a reverse way, for heating-responsive SME the photoreversible cross-links ensured the formation of the permanent domains, while PCL-based segments were used as the switching domains. Once more, the UV light illumination (cross-linking the BHECA segments) did not alter the crystalline features of the polyester precursors within PURs.

Other covalently crosslinked t-SMPs exhibiting 2W-SME were obtained with two semicrystalline polyester segments, that is, PCL and poly(ω-pentadecalactone) (PPDL).[31,32] From star-shaped precursors of PCL and PPDL as obtained by bulk ring-opening polymerization, Zotzmann et al. synthesized networks by condensation between these two polyester segments and a mixture of diisocyanates in dichloroethane.[31] As each crystallizable polyester segment possesses its own CIE and MIC, reversible t-SME was observed after both segments were oriented under constant stretching. In a second work, Behl et al.[32] investigated a particular programming process, which consisted to stretch out the networks made of both segments above their T_m, followed by a cooling step up to an intermediate temperature between T_m of PCL (≈60 °C) and PPDL (≈95 °C). Such process enabled to form a skeleton-like structure within these physically crosslinked materials in such a way that PCL got constrained to crystallize toward a chain-extended crystallization process and got actuated upon a 2W-SME by simply heating and cooling around its T_m.

The present study aims on exploring the strategy using photochemistry for the permanent network formation to design promising SMPs with both 2W-SME and t-SME. In contrast to submentioned studies, the herein chain-extension pathway combined both PCL and PPDL segments (heat-responsive segments) with BHECA (light-responsive moieties) into innovative PURs via the solvent-free reactive extrusion technology. This simple strategy might be considered extremely versatile and adaptive simply because of the possibility to vary the crystallizable segments, and the coupling agents, paving the way to the design of a multitude of triple (or more) shape-memory polymers with 2W behavior. Herein, the feasibility was confirmed using 1,6-hexamethylene diisocyanate as coupling agent. Once the permanent networks were set after light-induced [2+2] cycloaddition reactions, 1W- and 2W-SMEs of resulting PURs were then confirmed by DTMA measurements and correlated with their melting features using DSC and 2D wide angle X-ray scattering (WAXS) measurements.

2. Experimental Section

2.1. Materials

ω-Pentadecalactone (ω-PDL, ≥98%, Aldrich), 1,5,7-triazabicyclo[4.4.0]dec-5-ene (TBD, 98%, Aldrich), and 1,8-octane diol (99+%, Acros) were dried by three consecutive azeotropic distillations in toluene before use. α,ω-Dihydroxyl poly(ε-caprolactone) ($PCL(OH)_2$, Capa 2402, M_n = 4000 g mol^{-1}, $Đ$ = 1.48) was used as kindly supplied by Perstorp. As previously reported by Zotzmann et al.,[31] BHECA was obtained from methyl cinnamate and diethanolamine (VWR, for synthesis) via amminolysis reaction in the presence of sodium methoxide (30 wt% solution in methanol, Across). Hexamethylene diisocyanate (HMDI, Alfa Caesar) was stocked under inert atmosphere (glovebox) and used as received.

2.2. Synthesis of α, ω-Dihydroxyl Poly(ω-pentadecalactone) ($PPDL(OH)_2$)

$PPDL(OH)_2$ was obtained by ring-opening polymerization (ROP) of PDL initiated by 1,8-octanediol and catalyzed by TBD (1:1 molar ratio for [alcohol]/[TBD]. The synthesis was conducted in a 250 mL round-bottom glass reactor equipped with a nitrogen inlet, refrigerator, and a mechanical stirrer, beforehand conditioned under nitrogen flow at 100 °C for 1 h. ω-PDL (102.10 g, 0.4245 mol), 1,8-octanediol (3.59 g, 0.0245 mol), and TBD (3.41 g, 0.0245 g) were introduced under nitrogen flow in the reactor and the polymerization was performed under gentle stirring (50 rpm) at 100 °C for 48 h. The crude product was dissolved in a minimum volume of $CHCl_3$, followed by

precipitation into a sevenfold excess of heptane. $PPDL(OH)_2$ was then recovered by filtration and drying under reduced pressure to constant weight.

^1H NMR (500 MHz, $CDCl_3$, r.t.) (see Figure S1, Supporting Information): $-R-[-C(=O)-CH_2(a)-CH_2(b)-(CH_2(c)-CH_2(c))_5-CH_2(b)-CH_2(d)-O-]_n-C(=O)-CH_2(a)-CH_2(b)-(CH_2(c)-CH_2(c))_5-CH_2(b)-CH_2(d')-OH$: δ (ppm) = 4.05 (t, CH_2(d)), 3.63 (t, CH_2(d′)), 2.28 (t, CH_2(a)), 1.61 (brs, CH_2(b)), and 1.25 (brs, CH_2(c)).

2.3. Synthesis of PURs

PURs studied in this work were prepared by reactive extrusion using a 15 cm^3 co-rotating twin-screw DSM microcompounder. $PCL(OH)_2$ was first introduced at 40 °C and 30 rpm. Temperature was then increased to 80 °C for introducing BHECA and $PPDL(OH)_2$ successively. After stabilization of the torque values, HMDI was finally introduced (1.1 equiv. with respect to the overall hydroxyl content). The process was conducted at 130 °C and 75 rpm until reaching maximum torque values (or beyond the limits of the equipment), considering that the reaction was completed. The resulting PUR were hot-pressed (160 °C) for further characterization.

2.4. Characterization Techniques

Size-exclusion chromatography (SEC) of precursors was performed in chloroform (sample concentration: 1 wt%) at 30 °C using an Agilent liquid chromatograph equipped with an Agilent degasser, an isocratic HPLC pump (flow rate: 1 mL min^{-1}), an Agilent autosampler (loop volume = 200 µL, solution conc. = 2.5 mg mL^{-1}), an Agilent-DRI refractive index detector, and three columns: a PL gel 10 µm guard column and two PL gel Mixed-D 10 µm columns (linear columns for separation of Mw PS ranging from 500 to 10^6 g mol^{-1}). Molar mass and molar mass distribution were calculated by reference to a relative calibration curve from polystyrene standards. ^1H NMR spectrum of $PPDL(OH)_2$ was collected in $CDCl_3$ solution on a Bruker AMX-500 spectrometer with a frequency of 500 MHz. Thermal properties of precursors and PURs were determined by DSC measurements using a DSC Q200 from TA Instruments under nitrogen flow. The following "heat/cool/heat" procedure was applied to all samples: first heating to 200 °C (10 °C min^{-1}) in order to erase the thermal history of samples, cooling to –80 °C (10 °C min^{-1}), followed by a second heating to 200 °C (10 °C min^{-1}). Sample weights were generally in the range of 5–10 mg. ATR Fourier-transform infrared (FTIR) spectra were recorded using Bruker Tensor 17 spectrometer. The structural evolution during stretching to the temporary shape and the recovery to the initial shape was followed in situ by means of WAXS. Experiments were carried out using the synchrotron radiation on the D2AM beamline at ESRF (Grenoble, France). Acquisitions were performed in transmission mode using an energy of 10 keV. A home-made tensile stage was used to deform and heat the samples. One-way and two-way shape-memory properties were determined using the stress-controlled Q800 apparatus on rectangular specimens of ≈30 mm × 5 mm × 25 mm cut from hot-pressed films irradiated at long wavelengths (λ = 365 nm) with a UV lamp (Spectroline, model ENF-240 cm^3/FE, One 4-WBL, BLE-270W). Note that for each sample, a heating ramp (5 °C min^{-1}) and a cooling ramp (3 °C min^{-1}) were successively applied in order to limit the strain variation at high temperature. The typical four-step program was applied to determine the one-way behavior: (a) apply of a given load at a temperature higher than the second T_m of PUR system (T = 100 °C) to stretch the sample; (b) cooling in two steps to 60 °C and then to 0 °C (10 min isotherm) at 2 °C min^{-1} to fix the temporary shape; (c) quick unloading; (d) final heating to 100 °C at 3 °C min^{-1} to let the sample recovered to its initial shape. The one-way SME was characterized by the shape fixity ratio R_f, representing the ability to maintain temporary shape and by shape recovery ratio R_r, which shows the extent of the recovery, as defined

$$R_f\ (\%) = \left(\frac{\varepsilon_{un}}{\varepsilon_{max}}\right) \quad (1)$$

$$R_r\ (\%) = \left(\frac{\varepsilon_{un} - \varepsilon_{fin}}{\varepsilon_{un}}\right) \quad (2)$$

where ε_{un} is the strain after cooling and unloading, ε_{max} is the strain obtained before the constant loading was released, and ε_{fin} is the strain obtained after heating in the step of recovery.

To evaluate the two-way SME, this corresponding cycle was slightly modified: a constant stress was maintained after the fixation of the temporary shape, prior to reheating. Increment in strain during the cooling under constant load is defined by the so-called actuation magnitude R_{act}(%). The strain recovery magnitude R_{rec}(%) is evaluated after the second heating. They were determined as follows[19,21,22]

$$R_{act}\ (\%) = \left(\frac{l_{low} - l_{high}^{initial}}{l_0}\right) (\text{or } \varepsilon_{low} - \varepsilon_{high}) \quad (3)$$

$$R_{rec}\ (\%) = \left(\frac{l_{low} - l_{high}^{final}}{l_{low} - l_{high}^{initial}}\right) \quad (4)$$

where l_0, l_{low}, $l_{high}^{initial}$, and l_{high}^{final} were the initial length between the DMTA clamps, length at the lowest temperature at full elongation, length at high temperature before elongation, and length at high temperature after contraction under loading, respectively.

3. Results and Discussion

In order to develop new simple, versatile, and adjustable strategy to design a multitude of triple (or more) shape-memory polymers with 2W behavior, chain-extension reaction between α,ω-diol polyesters (i.e., $PCL(OH)_2$ and $PPDL(OH)_2$), BHECA monomer, and an aliphatic diisocyanate as coupling agent, was exploited to synthesize a series of PURs as t-SMPs with desired 2W-SME (**Figure 1**). While $PCL(OH)_2$ oligomers

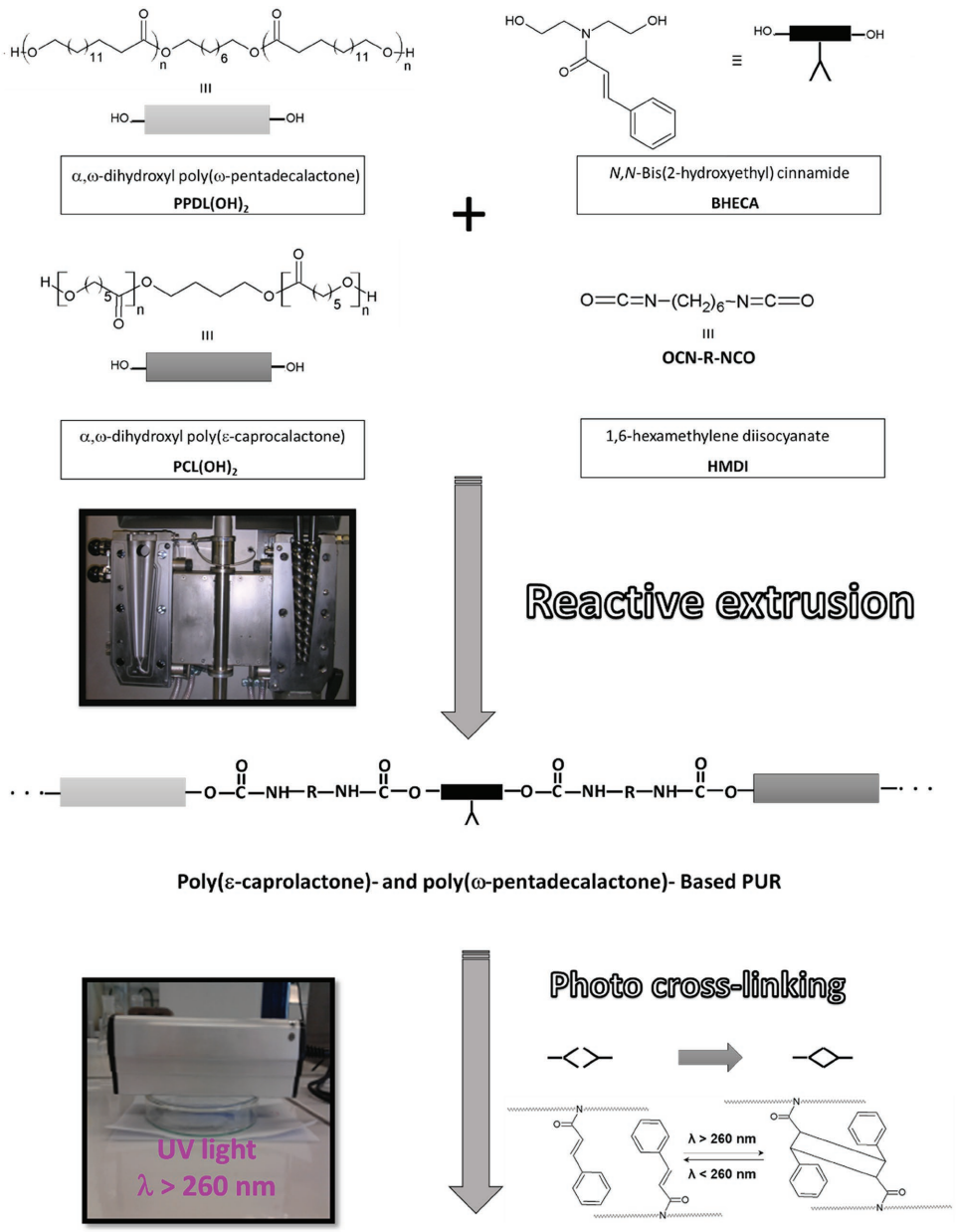

Figure 1. Schematic pathway followed to obtain PURs with 1W-SME and 2W-SME properties.

are commercially available, $PPDL(OH)_2$ was obtained by TBD-catalyzed ring-opening polymerization of ω-PDL, as initiated from 1,8-octanediol at 100 °C for 48 h (**Scheme 1**). [1,8-Octane diol)]/[TBD] ratio of 1 was selected following the Bouyahyi's results of about bulk ω-PDL polymerization initiated from benzyl alcohol.[33] ^{1}H NMR of crude product (see Figure S1, Supporting Information) did not exhibit any proton signal relative to $-C(=O)OCH_2-$ of the monomer unit (δ = 4.15 ppm), attesting for the full conversion of ω-PDL into polymer. For the recovered $PPDL(OH)_2$, SEC analyses carried out in chloroform (upon PS calibration) showed a $\bar{M}_n$ of 9400 g mol^{-1} associated with a dispersity of 1.6 and DSC analysis revealed a T_m of around 94 °C (with a melting enthalpy (ΔH_m) of 149 J g^{-1}).

In a subsequent way, different PUR networks were synthesized after coupling reactions between BHECA (80 relative polyester mol%) and HMDI (1.1 eq. with respect to total OH functions) by varying the weight composition between $PCL(OH)_2$ and $PPDL(OH)_2$ oligomers.

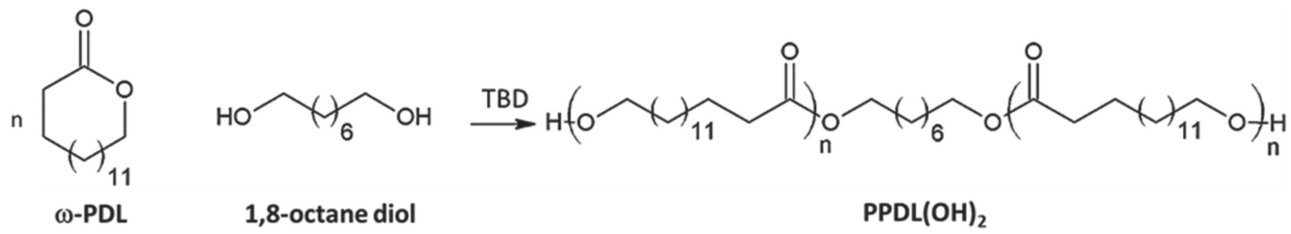

Scheme 1. Synthesis of α,ω-dihydroxyl poly(ω-pentadecalactone) as obtained by ROP of ω-PDL initiated by 1,8-octane diol.

They are abbreviated as $PUR_{[x/(y/z)]}$ where x, y, and z represent the polyester molar content, $PCL(OH)_2$ and $PPDL(OH)_2$ weight contents, according to their respective compositions detailed in **Table 1**. It is worth noting that the molar content of BHECA (80 mol%) was selected based on previous studies[29] ($PUR_{[20/(100/0)]}$, Table 1), and used in all PCL-, PPDL-, and PCL/PPDL-based PURs. The PCL content was kept above 50 wt% in order to ensure crystallization induced upon elongation.

As previously demonstrated by some of us, PURs suffered from a lack of solubility in any solvent (e.g., chloroform, toluene, tetrahydrofuran) due to the importance of hydrogen bonding, making molecular characterizations via SEC and ^{1}H NMR techniques impossible. The simplest way to highlight the efficiency of chain-extension reactions was based on FTIR technique. The most striking feature on FTIR spectra of PURs (**Figure 2**, for $PUR_{[20/(50/50)]}$) is the absence of band (2200–2300 cm^{-1}), ascribed to the urethane functionality. The stretching vibration band (1720 cm^{-1}) of carbonyl ester linkage, the stretching and bending vibration bands at 1550–1650 cm^{-1} from amide of urethane linkage are also noted.

Regarding the thermal properties, commercial $PCL(OH)_2$ exhibited a T_m at around 50 °C and the here-obtained $PPDL(OH)_2$ at 94 °C. DSC analyses of neat polyesters PURs (Table 1, $PUR_{[20/(100/0)]}$ and $PUR_{[20/(0/100)]}$) showed that both PCL and PPDL crystal properties are insignificantly influenced. Concerning the PURs containing both PCL and PPDL segments (Table 1, $PUR_{[20/(50/50)]}$, $PUR_{[20/(75/25)]}$), the presence of two T_m in the same range as the neat precursors is observed, suggesting that the semicrystalline properties of both PCL and PPDL are maintained. Exceptionally, a slight decrease in ΔH_m for the PPDL sequences might be suggested at lower PPDL content ($PUR_{[20/(75/25)]}$). However, further discussion of a possible tendency must be avoided as there are not enough data to conclude. As discussed before, the PCL content was kept above 50 wt% in order to ensure crystallization induced upon elongation.

The materials were further photochemically crosslinked by irradiation of compression-molded films at $\lambda > 254$ nm for 2 h. This important step enables the formation of the permanent domains derived from these cinnamate BHECA moieties after undergoing [2+2] cycloaddition at this wavelength.[29] 1W-SME (heat-responsive) was demonstrated for all PURs using DMTA equipment. Before applying the typical four-step mechanical cycle to specimens (see the Experimental Section), a first heating step directly followed by a cooling step was programmed in order to erase the "thermomechanical" history of the compressed films. In a subsequent step, the samples were stretched to a given elongation between 60 and 100% (= ε_{max}) at a temperature just above the second T_m of PURs, that is, at 92 °C by applying a constant deformation stress. This loading was maintained during cooling to 0 °C to achieve the temporary shape and then released. From this state characterized with a certain elongation (ε_{un}), the final shape was recovered to a final elongation (ε_{fin}) by a second heating to 95 °C. As illustrated by the R_f and R_r ratios (**Table 2**), defining the ability to fix temporary shape and to recover initial shape, good 1W-SME was observed for the PURs. This was further supported by the thermomechanical cycles of $PUR_{[20/(50/50)]}$ as illustrated in **Figure 3**. As seen, $PUR_{[20/(50/50)]}$ underwent an increase in strain occurring at 70 °C, which is close to the T_c of PPDL segment (between 71.5 and 78 °C), during the cooling step. $PUR_{[20/(100/0)]}$, only made from PCL segments,

Table 1. Compositions of various PURs and their respective thermal properties.

Code	[Polyesters]/[BHECA] [mol%/mol%]	$PCL(OH)_2$/$PPDL(OH)_2$ [wt%/wt%]	Conv[a] [%]	PCL segment				PPDL segment			
				T_{c1}[b] [°C]	ΔH_{c1}[b] [J g^{-1}]	T_{m1}[c] [°C]	ΔH_{m1}[c] [J g^{-1}]	T_{c2}[b] [°C]	ΔH_{c2}[b] [J g^{-1}]	T_{m2}[c] [°C]	ΔH_{m2}[c] [J g^{-1}]
$PUR_{[20/(100/0)]}$[d]	20/80	100/0	100	23	49.51	53	52.13	–	–	–	–
$PUR_{[20/(50/50)]}$	20/80	50/50	100	18	50.30	44	49.56	76	107.6	89	105.2
$PUR_{[20/(75/25)]}$	20/80	75/25	100	15	45.38	49	50.02	73	79.70	88	87.45
$PUR_{[40/(75/25)]}$	40/60	75/25	100	21	43.13	50	49.58	62	82.50	87	80.83
$PUR_{[20/(0/100)]}$	20/80	0/100	100	/	/	/	/	78	108.4	90	119.9

[a]As determined by FTIR measurements; [b]Recalculated according to the relative polyester content from DSC measurements (from 200 to 0 °C (10 °C min^{-1}); cooling cycle); [c]Recalculated according to the relative polyester from the DSC measurements (from –80 to 200 °C (10 °C min^{-1}); second heating cycle); [d]Data obtained in a previous work.[25]

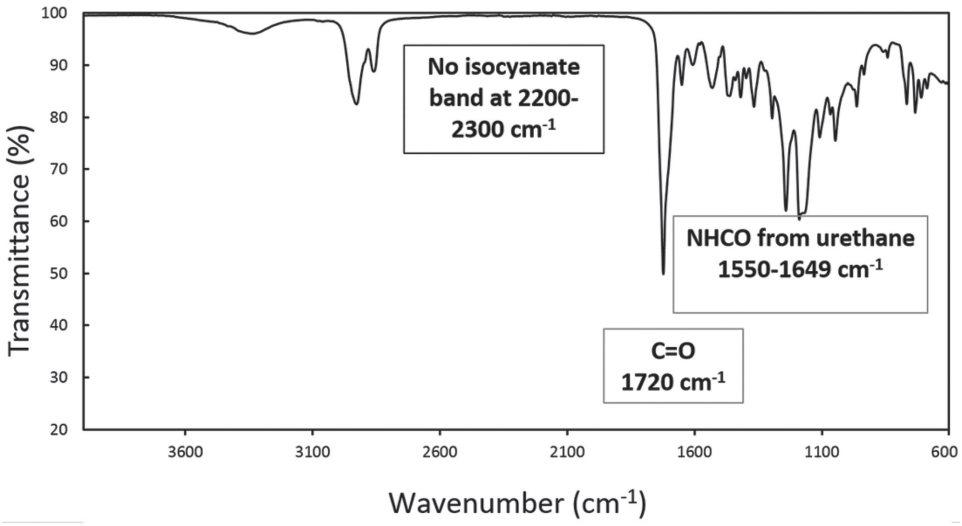

Figure 2. FTIR spectrum of $PUR_{[20/(50/50)]}$.

exhibits a similar behavior due to rearrangement of PCL crystalline phase under stress. In this case, increase and decrease in strain were observed from 20 °C (close to T_c of semicrystalline PCL-based segment) during cooling step and 50 °C (close to T_m) in second heating step, respectively. The same strain increment is observed in the curve respective to the PPDL-based $PUR_{[20/(0/100)]}$. Such behavior is ascribed due to the growth of crystallites under stress responsible for the CIE phenomenon.[31] As expected for 1W-SMPs, the recovery step of $PUR_{[20/(50/50)]}$ proceeded in a single step. The large decrease in strain was observed once the heating temperature reached 80 °C, which corresponds to the onset of melting range of PPDL segment. Both strain increments respective to their respective polyester segments became well-observed only in the case of PU $PUR_{[20/(75/25)]}$ where PCL content increased to 75 wt%. Two independent CIE thereby appeared during the cooling step as shown in the thermomechanical curve for $PUR_{[20/(75/25)]}$ (Figure 3). It is worth mentioning that CIE respective to PPDL segment is less pronounced than for $PUR_{[20/(50/50)]}$ due to the lower PPDL weight fraction. Interestingly, $PUR_{[20/(75/25)]}$ recovered to its initial shape following two successive decreases in strain, related to the T_m of each polyester segment. On thermomechanical curves presented in Figure 3, both strain increment and decrement are indicated with an arrow. In this approach, the exhibited CIE phenomena and the two-step recovery demonstrate that the obtained photo-crosslinked semicrystalline-based PURs maintain the crystalline features of their respective precursors.

Table 2. Shape-memory parameters of PURs determined after classical 1W-SME programming and recovery processes.

Entry	PCL wt%	σ_{app} [a] [MPa]	ε_{ext} [%]	R_f [b] [%]	R_r [b] [%]
$PUR_{[20/(100/0)]}$	66	0.1	80	100	100
$PUR_{[20/(50/50)]}$	35	0.06	100	100	100
$PUR_{[20/(75/25)]}$	52	0.6	65	100	100
$PUR_{[40/(75/25)]}$	63	0.6	120	100	100
$PUR_{[20/(0/100)]}$	–	0.02	100	100	100

[a]The specific stress applied was chosen in order to keep the ε_{ext} between 60 and 120% for all the materials; [b]As determined by R_f (%) = $\varepsilon_{un}/\varepsilon_{max}$ and Rr (%) = $(\varepsilon_{un} - \varepsilon_{fin})/\varepsilon_{un}$ where ε_{un} is the strain after cooling to 0 °C and unloading, ε_{max} is the strain obtained before the constant loading was released at 0 °C, and ε_{fin} is the strain obtained after second heating to 100 °C (above both PCL and PPDL melting).

Following our statements, the 2W-SMPs of the here-obtained photo-crosslinked PURs were evaluated. The studies were realized on the $PUR_{[20/(75/25)]}$ due to its ability to display two different CIE respective to each polyester segment during programming. These increments in strain being related to the relative crystallinity of the PUR (presence of melting enthalpies even under stress), especially for the PCL segments. Thermomechanical cycle was first adapted in order to check whether well-known 2W-actuation from PCL semicrystalline segment was still observed up to 60 °C, that is, below T_m of PPDL segment. After stretching at T_{high} (100 °C), samples were cooled at 2 °C min^{-1} to 60 °C followed by three successive cycles of cooling (2 °C min^{-1}) and heating (3 °C min^{-1}) between 0 and 60 °C, without removing external stress applied to the deformed films. While the first cycle of heating/cooling served to erase the thermal history of PUR, the second and the third cycles were practically repeatable in terms of actuation strain (**Figure 4**, where the second cycle is highlighted in 2D curve of strain vs temperature). R_{act} (%) and R_{rec} (%) ratios, giving strain increment amplitude during actuation and actuation efficiency, are reported in **Table 3**. R_{act} was 7% and an incomplete R_{rec} of 70% were obtained for $PUR_{[20/(75/25)]}$.

In order to improve recovery ratio, a sample containing lower amount of BHECA and higher polyester content was prepared ($PUR_{[40/(75/25)]}$). While these PUR thermal properties (Table 1) and heating-responsive 1W-SME (Table 2) differ insignificantly from those of $PUR_{[20/(75/25)]}$, a complete recovery R_{rec} was achieved for $PUR_{[20/(0/100)]}$. Moreover, R_{act} expanded to 10%, most probably due to higher PCL content (higher total polyester content) in comparison to $PUR_{[20/(75/25)]}$.

Macromolecular Chemistry and Physics
www.mcp-journal.de

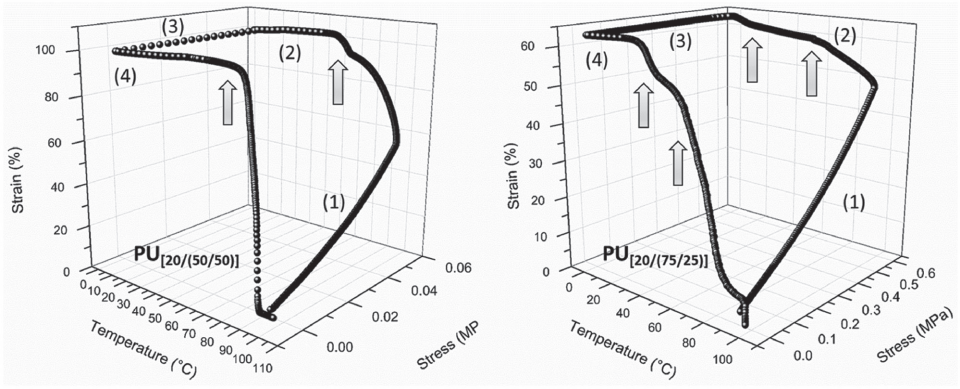

Figure 3. Four-step thermomechanical processes obtained by DMTA for $PUR_{[20/(50/50)]}$ and $PUR_{[20/(75/25)]}$. (1) Deformation: constant loading at 100 °C; (2) Fixing: cooling (2 °C min^{-1}) to 60 °C and then to 0 °C; (3) Unloading: unloading at 0 °C; (4) Recovery: heating (3 °C min^{-1}) to 100 °C.

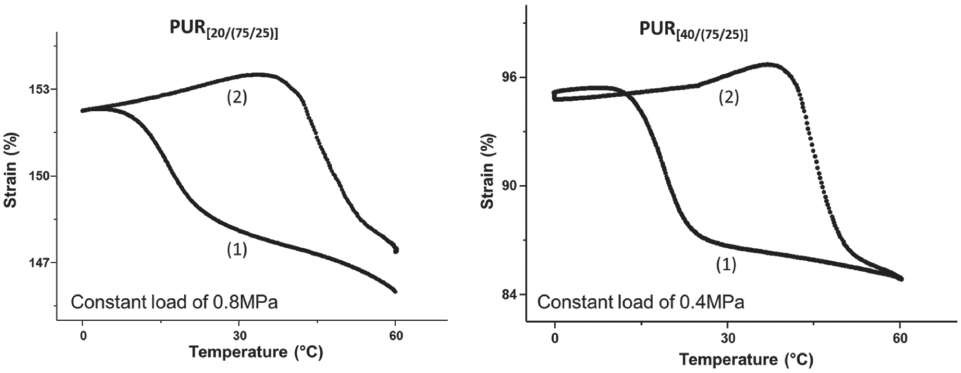

Figure 4. Second cycle of DTMA process showing reversibility between 0 and 60 °C for $PUR_{[20/(75/25)]}$ (left) or $PUR_{[40/(75/25)]}$ (right). (1) Cooling (under constant stress); (2) Heating (under constant stress).

Both t-SME and 2W-SME were explored for both polyester segments where the actuation investigation was carried out above T_m of PPDL. Like our previous experiments, cooling and heating processes were successively applied on elongated films, still under constant load but in a range of temperatures between 0 and 100 °C. As seen in the second cycles shown in **Figure 5**, two CIE were observed during cooling step, CIE respective to PCL segment being less pronounced than the one associated to PPDL segment for $PUR_{[20/(75/25)]}$ and inversely in $PUR_{[40/(75/25)]}$. We have to mention that a good reproducibility was achieved by repeating the actuation program three times. Again, this indicates a certain dependence on actuation upon the weight ratio of each polyester segment into PURs, and therefore of their melting properties and crystallinity degrees. Although R_{act} was of 85% for $PUR_{[40/(75/25)]}$, R_{rec} was of only 50%. Recovery reached 62% for $PUR_{[20/(75/25)]}$ while R_{act} was less pronounced (47%). As mentioned in the Introduction, Zotzmann et al. already published a very impressive work about reversible actuation of both types of semicrystalline segments.[31] Two of their copolymer networks obtained by solvent-way, containing 50 wt% of PCL, exhibited a completely reversible triple-shape effect. By applying a constant load of 0.6 MPa (and 1.0 MPa for other samples), samples stretched from 25% of strain to 35% after cooling from 100 to 0 °C (and to 50%, for other samples) within two shapes present at each switching temperature. Recovery upon heating ramp proceeded in two steps to an initial strain of 25%. By comparison to the work by Zotzmann et al. and although our $PUR_{[20/(75/25)]}$ and $PUR_{[40/(75/25)]}$, obtained in bulk via an interesting pathway, did not totally recover to the same strain before the cooling rate, they still exhibit both

Table 3. Actuation parameters of $PUR_{[20/(75/25)]}$ and $PUR_{[40/(75/25)]}$ relative to PCL segment and relative to a total actuation associated to a t-SME.

Entry	PCL actuation			Polyesters (PCL and PPDL) actuation		
	σ_{app} [MPa]	R_{act} [a,b) [%]	R_{rec} [a,b) [%]	σ_{app} [MPa]	R_{act} [a,c) [%]	R_{rec} [a,c) [%]
$PUR_{[20/(75/25)]}$	0.8	7	70	0.8	58	62
$PUR_{[40/(75/25)]}$	0.4	10	100	0.4	85	50

[a)]Values obtained at the second actuation cycle; [b)]As determined by R_{act} (%) = $(l_{low} - l_{high}^{initial})/l_0$ and R_{rec} (%) = $(l_{low} - l_{high}^{final})/(l_{low} - l_{high}^{initial})$ where l_0, l_{low}, $l_{high}^{initial}$, and l_{high}^{final} were initial length between the DMTA clamps, length at 0 °C at full elongation, length at 60 °C before elongation, and length at 60 °C after contraction under loading; [c)]As determined by R_{act} (%) = $(l_{low} - l_{high}^{initial})/l_0$ and R_{rec} (%) = $(l_{low} - l_{high}^{final})/(l_{low} - l_{high}^{initial})$ where l_0, l_{low}, $l_{high}^{initial}$, and $l_{high}^{initial}$ were initial length between the DMTA clamps, length at 0 °C at full elongation, length at 100 °C before elongation, and length at 100 °C after contraction under loading.

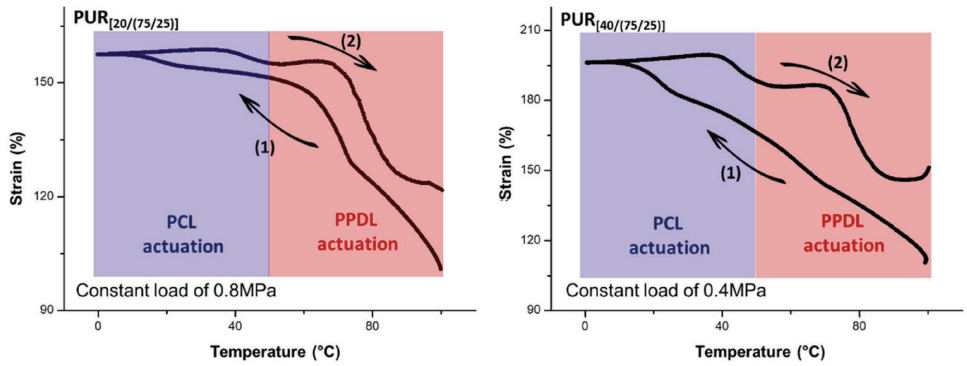

Figure 5. Second cycle of DTMA process showing reversibility between 0 and 100 °C for $PUR_{[20/(75/25)]}$ (left) or $PUR_{[40/(75/25)]}$ (right). (1) Cooling (under constant stress); (2) Heating (under constant stress).

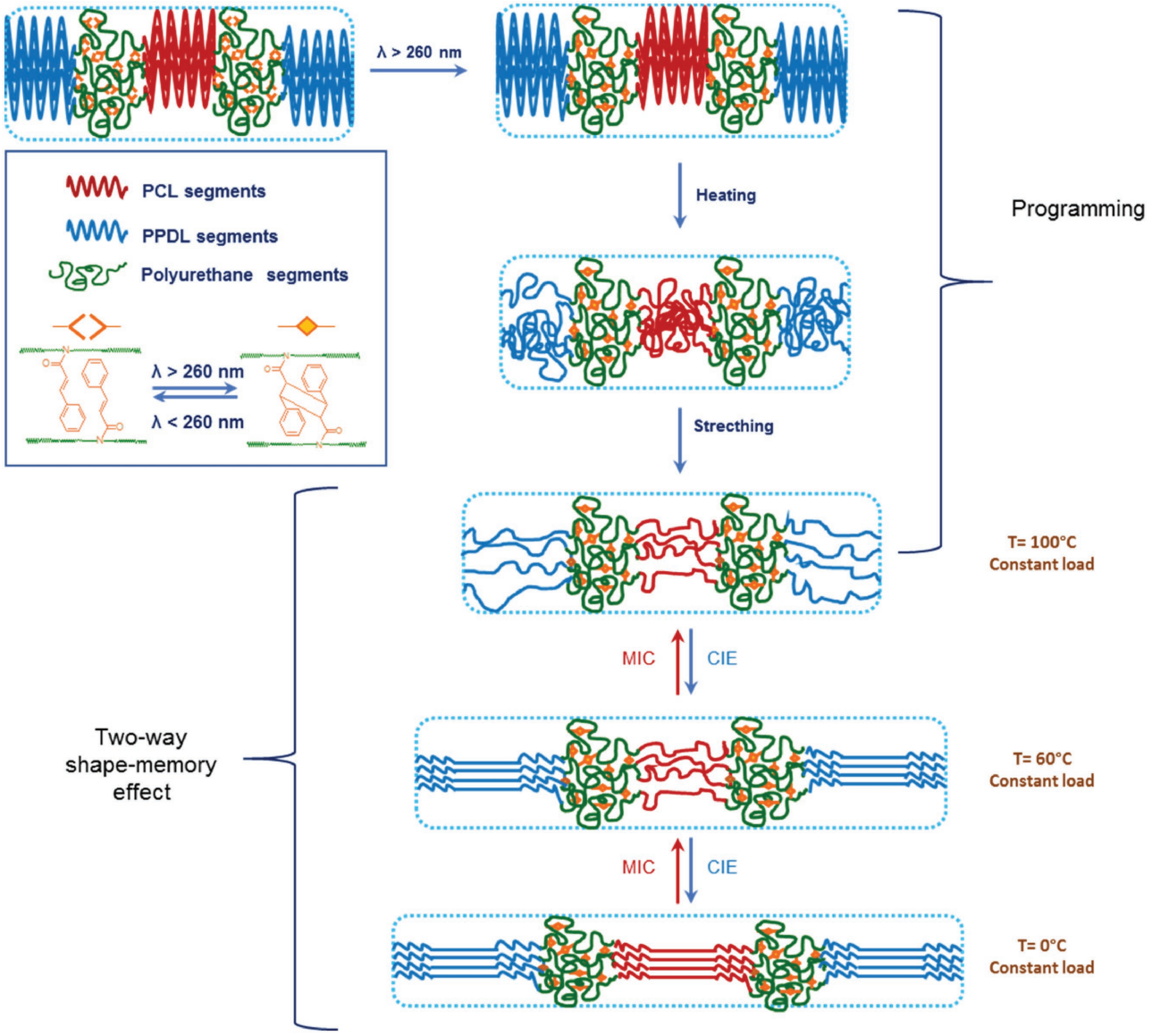

Figure 6. Schematic representation of the programming and the subsequent 2W-SME applied to the PCL-PPDL-based PURs.

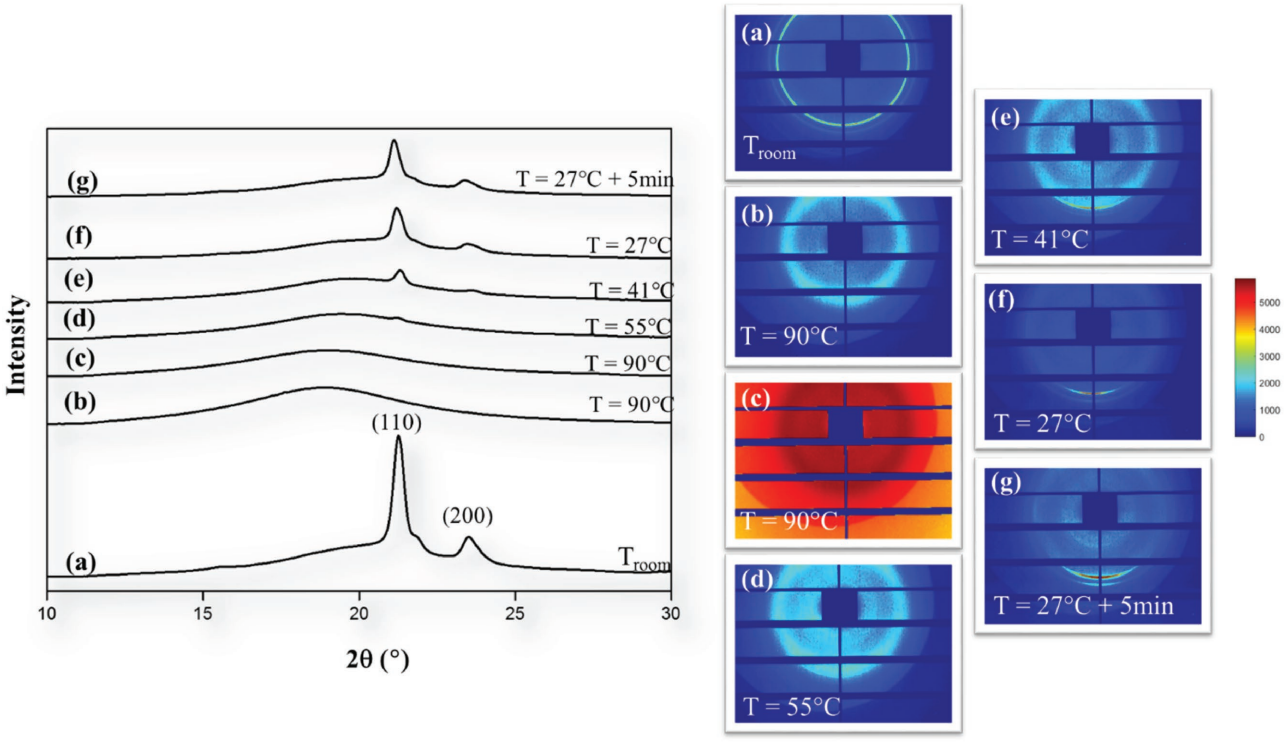

Figure 7. WAXS intensity profiles (left) and 2D WAXS patterns (right) of $PUR_{[40/(75/25)]}$: a) undeformed compressed film at room temperature, b) undeformed film at 90 °C, c) stretched film (elongation of 100%) at 90 °C, d) stretched film at 55 °C, e) stretched film at 41 °C, f) stretched film at 27 °C, and g) stretched film stayed 5 min at 27 °C.

t-SME and 2W-actuation. In addition, the strain increment of our promising samples was larger than those mentioned at the same range of applied constant. Furthermore, it can be suggested that the formation of an internal skeleton under stress happened in our novel PURs in the same way that the PCL and PPDL-based copoly(ester-urethane) network recently developed by Behl et al.[32] Indeed, PPDL was first able to crystallize under a certain stress due to an adapted programming process, followed by the crystallization of the PCL segment. As PCL was constrained to crystallize toward the chain-extended crystallization process, the network can be actuated upon 2W-SME. In addition, it can be assumed that a (pre)skeleton made of PPDL is formed during the cooling of molded films, leading to crystallization of PCL segments following the deformation direction. The molecular reorientations of our system observed both in CIE and MIC processes are schematically described in **Figure 6**.

Microstructural behavior was studied by 2D WAXS measurements of $PUR_{[20/(100/0)]}$, $PUR_{[40/(75/25)]}$, and $PUR_{[20/(0/100)]}$. In the same manner the thermomechanical cycles are used during the DMA analyses, cross-linked films were put in an oven at 100 °C, following by cooling to room temperature, in order to erase the thermal history set by the compression molding and the subsequent UV illumination. It is well-known that PCL displays a sharp peak at 2θ around 21° and a lower intensity peak at 2θ around 23.8°, ascribed to the (110) and (200) planes, respectively.[34,35] In a similar way, the two main equatorial peaks of PPDL are recorded at nearly the same positions.[36] In this respect, only two peaks were observed for the PCL and PPDL-based PURs, that is, $PUR_{[40/(75/25)]}$ chosen as an example. Using a specific heating and tensile equipment, the crystalline deformations of the PURs were thus explored through WAXS observations. Thereby, the crosslinked films (obtained by compression and subsequent UV illumination) were mounted between two clamps and data were recorded during the course of the process, consisting of heating the films from room temperature to 90 °C, to subsequently stretch up to a strain of 100% and to cool down at 5 °C min^{-1} to room temperature under the fixed load. Only the WAXS profile and patterns of the $PUR_{[40/(75/25)]}$ are illustrated in **Figure 7**. As can be seen the sample is initially semicrystalline and exhibits an isotropic structure. When heated up to 90 °C, the sample became amorphous due to the melting of both PCL and PPDL crystals.

It can be noticed that whichever sample is tested, the peaks related to the diffraction pattern from crystals (either PCL either PPDL) of the polyester segments disappeared above the melting temperature, that is, 90 °C (see curve (b) in Figure 7). In agreement with the respective T_c of $PUR_{[20/(100/0)]}$ (only PCL-based) and $PUR_{[20/(0/100)]}$ (only PPDL-based) determined by DSC, WAXS results indicate that these peaks slowly reappear from 30 and 61 °C, respectively.

For the $PUR_{[40/(75/25)]}$, as shown in Figure 7, the intensity of these peaks slowly increases again from 55 °C and more obviously at 41 °C, indicating the growth of new oriented crystallites ascribed to the crystallization of PPDL. The low content in PPDL explains the weak intensity of these peaks at temperature lower than the T_c of PPDL. For temperatures below 30 °C a noticeable increase of the diffraction peaks intensity is observed and ascribed to the crystallization of PCL. This sharp increase

is explained by the fact that this PUR was mainly enriched in PCL domains (63% wt).

Nevertheless, the ability of the PPDL to first crystallize under a stress was confirmed by the study of $PUR_{[20/(0/100)]}$. In addition, the variation in the starting temperature of crystallization (and therefore the level in CIE) recorded for this tensile heating equipment could be simply explained by the slightly higher cooling rate used during the WAXS experiments.

Finally, as previously mentioned, the WAXS diffraction pattern in the angular range up to $2\theta = 35°$ of the unstretched sample (see Figure 7a) shows diffraction rings located at $2\theta = 21°$ and 23° indicating that the crystalline structure of the material is anisotropic. By contrast, the 2D diffraction patterns recorded during the cooling upon the applied deformation show the presence of diffraction arcs rather than rings. This confirms the oriented crystallization of the soft segments as shown by the presence of discontinuous Debye rings. It is worth mentioning that the orthorhombic structure of the crystal phases remained unchanged with the heating/cooling process, as no change along 2θ was noticed.

4. Conclusions

Novel photo-crosslinked semicrystalline PURs made of α,ω-diol PCL and PPDL segments were successfully obtained by reactive extrusion processing. While commercially available α,ω-diol PCL was used, α,ω-diol PPDL was synthesized by ring-opening polymerization performed in bulk, that is, in absence of any solvent, and using TBD as organic catalyst. Chain-extension reactions were performed at 130 °C between both polyester segments and in presence of BHECA monomer as photoreversible cross-linker using 1,6-hexamethylene diisocyanate as coupling agent. Subsequent UV light illumination of PUR films led to the formation of cycloadducts, acting as permanent domains. Interestingly, this latest innovative strategy proved efficient to maintain the crystallinity characteristic of the two polyester segments, that is, PCL and PPDL, into the resulting PURs. As a consequence, semicrystalline PURs exhibited two corresponding T_m at around 50 and 90 °C. Depending on the weight fraction between the polyester segments, triple and two-way shape-memory behaviors could be evidenced as demonstrated by DTMA measurements. This very simple and efficient strategy based on reversible photochemistry and coupling reaction directly performed by a solventless extrusion technique, could be adapted using other types of crystallizable segments, paving the way to the design of new triple (or more) shape-memory polymers with two-way behavior.

Supporting Information

Supporting Information is available from the Wiley Online Library or from the author.

Acknowledgements

LPCM thanks the Belgian Federal Government Office of Science Policy (SSTC-PAI 6/27) for general support and is much indebted to both Wallonia and the European Commission "FSE and FEDER" for financial support in the frame of Phasing-out Hainaut. F.P. is a FRS-FNRS research fellow and J.-M.R. is a FRS-FNRS research associate. The authors are indebted to the ESRF Synchrotron Facility (Grenoble, France) for beam time allocation on the D2AM beamline. The authors especially thank Dr. Morfin for her help during the experiments and data treatment. Financial support from the Wallonia and European Commission in the frame of the SINOPLISS-POLYEST and the LCFM-BIOMASS-BIOMAT_1 projects is gratefully acknowledged.

Conflict of Interest

The authors declare no conflict of interest.

Keywords

dual shape-memory 1W and 2W-effects, photo-crosslinking, semicrystalline polyester

Received: July 6, 2017
Revised: September 20, 2017
Published online:

[1] F. Pilate, A. Toncheva, P. Dubois, J.-M. Raquez, *Eur. Polym. J.* **2016**, *80*, 268.
[2] Q. Zhao, H. J. Qi, T. Xie, *Prog. Polym. Sci.* **2015**, *49*, 79.
[3] J. Hu, H. Meng, G. Li, S. I. Ibekwe, *Smart Mater. Struct.* **2012**, *21*, 053001.
[4] L. Santo, F. Quadrini, A. Accettura, W. Villadei, *Proc. Eng.* **2014**, *88*, 42.
[5] L. Yanju, D. Haiyang, L. Liwu, L. Jinsong, *Smart Mater. Struct.* **2014**, *23*, 023001.
[6] Q. Zhao, M. Behl, A. Lendlein, *Soft Matter* **2013**, *9*, 1744.
[7] T. Pretsch, *Smart Mater. Struct.* **2010**, *19*, 015006.
[8] T. Xie, X. Xiao, Y. T. Cheng, *Macromol. Rapid Commun.* **2009**, *30*, 1823.
[9] X. Luo, P. T. Mather, *Adv. Funct. Mater.* **2010**, *20*, 2649.
[10] S. Chen, J. Hu, C.-W. Yuen, L. Chan, H. Zhuo, *Polym. Adv. Technol.* **2010**, *21*, 377.
[11] C. Y. Bae, J. H. Park, E. Y. Kim, Y. S. Kang, B. K. Kim, *J. Mater. Chem.* **2011**, *21*, 11288.
[12] L. Xiao, M. Wei, M. Zhan, J. Zhang, H. Xie, X. Deng, K. Yang, Y. Wang, *Polym. Chem.* **2014**, *5*, 2231.
[13] M. Wei, M. Zhan, D. Yu, H. Xie, M. He, K. Yang, Y. Wang, *ACS Appl. Mater. Interfaces* **2015**, *7*, 2585.
[14] I. Bellin, S. Kelch, R. Langer, A. Lendlein, *Proc. Natl. Acad. Sci. USA* **2006**, *103*, 18043.
[15] Y. Luo, Y. Guo, X. Gao, B.-G. Li, T. Xie, *Adv. Mater.* **2013**, *25*, 743.
[16] T. Xie, *Nature* **2010**, *464*, 267.
[17] C. Samuel, S. Barrau, J.-M. Lefebvre, J.-M. Raquez, P. Dubois, *Macromolecules* **2014**, *47*, 6791.
[18] D. Thomsen III, P. Keller, J. Naciri, R. Pink, H. Jeon, D. Shenoy, B. Ratna, *Macromolecules* **2001**, *34*, 5868.
[19] W. Li, Y. Liub, J. Leng, *RSC Adv.* **2014**, *4*, 61847.
[20] H. Qin, P. T. Mather, *Macromolecules* **2009**, *42*, 273.
[21] J. Küpfer, H. Finkelmann, *Makromol. Chem., Rapid Commun.* **1991**, *12*, 717.
[22] J. Küpfer, H. Finkelmann, *Macromol. Chem. Phys.* **1994**, *195*, 1353.
[23] S. Pandini, S. Passera, M. Messori, K. Paderni, M. Toselli, A. Gianoncelli, E. Bontempi, T. Riccò, *Polymer* **2012**, *53*, 1915.
[24] K. Ishida, N. Yoshie, *Macromolecules* **2008**, *41*, 4753.

[25] T. Chung, A. Romo-Uribe, P. T. Mather, *Macromolecules* **2008**, *41*, 184.
[26] J.-M. Raquez, S. Vanderstappen, F. Meyer, P. Verge, M. Alexandre, J.-M. Thomassin, C. Jérôme, P. Dubois, *Chem. Eur. J.* **2011**, *17*, 10135.
[27] I. Chodak, *Prog. Polym. Sci.* **1998**, *23*, 1409.
[28] A. J. J. Peacock, *Macromol. Sci. Polym. Rev. C* **2001**, *41*, 285.
[29] F. Pilate, R. Mincheva, J. De Winter, P. Gerbaux, L. Wu, R. Todd, J.-M. Raquez, P. Dubois, *Chem. Mater.* **2014**, *26*, 5860.
[30] C. Jin, X. Sun, L. Wu, *Des. Monomers Polym.* **2011**, *14*, 47.
[31] J. Zotzmann, M. Behl, D. Hofmann, A. Lendlein, *Adv. Mater.* **2010**, *22*, 3424.
[32] M. Behl, K. Kratz, J. Zotzmann, U. Nöchel, A. Lendlein, *Adv. Mater.* **2013**, *25*, 4466.
[33] M. Bouyahyi, M. P. F. Pepels, A. Heise, R. Duchateau, *Macromolecules* **2012**, *45*, 3356.
[34] V. Correlo, L. Boesel, M. Bhattacharya, J. Mano, N. Neves, R. Reis, *Mater. Sci. Eng., A* **2005**, *403*, 57.
[35] S. Gautam, A. K. Dinda, N. C. Mishra, *Mater. Sci. Eng., C* **2013**, *33*, 1228.
[36] M. Gazzano, V. Malta, M. L. Focarete, M. Scandola, R. A. Gross, *J. Polym. Sci., Part B: Polym. Phys.* **2003**, *41*, 1009.

